published by Ural Federal University
eISSN 2411-1414
chimicatechnoacta.ru

ARTICLE
2023, vol. 10(3), No. 202310315
DOI: 10.15826/chimtech.2023.10.3.15

Structural transformations and their impact on the mechanical and antifriction properties in the process of alloying graphitized hypereutectoid steel with copper

Natalia V. Stepanova *, Elena A. Lozhkina

Faculty of Mechanical Engineering and Technologies, Novosibirsk State Technical University, Novosibirsk 630073, Russia
* Corresponding author: stepanova@corp.nstu.ru

This paper belongs to the RKFM'23 Special Issue: https://chem.conf.nstu.ru/.
Guest Editors: Prof. N. Uvarov and Prof. E. Aubakirov.

Abstract

The purpose of the work is to develop a cast antifriction material based on an iron-carbon alloy with a high copper content for use in large, heavy duty sliding friction units. Using the casting method in self-hardening liquid glass mixtures, two specimens of hypereutectoid graphitized steel with different copper contents (0.09 and 8.76 wt.%) were produced. To obtain graphite in the steel structure, modification with the silicocalcium (SiCa) was used. The microstructural examination was carried out using optical metallography, SEM and TEM methods. The impact of copper on the structure as well as the mechanical and antifriction properties of graphitized hypereutectoid steel was studied. It was found that adding 8.76 wt.% of copper to the steel composition leads to an increase in the Brinell hardness level of the material from 250 to 300 HB, ultimate tensile strength from 250 to 380 MPa and compressive strength from 1050 to 1200 MPa, which is associated with an increase in the microhardness of pearlite from 350 to 420 HV. To assess the impact of copper on the sliding friction coefficient of graphitized hypereutectoid steel, a curve of sliding friction coefficient vs applied load was plotted; the experiment was carried out according to the liner-on-disk scheme. The wear resistance of materials under sliding friction conditions was also assessed using this method. Copper alloying has a positive effect on the wear resistance of graphitized hypereutectoid steel by increasing the mechanical properties of the material and also by reducing the level of the sliding friction coefficient under boundary lubrication conditions.

Keywords

graphitized hypereutectoid steel
structure
ε-Cu phase
mechanical properties
antifriction properties

Received: 15.09.23
Revised: 30.09.23
Accepted: 16.10.23
Available online: 20.10.23

Key findings

- An antifriction material based on graphitized hypereutectoid steel with a high copper content was developed.
- Adding copper to graphitized hypereutectoid steel leads to an increase in the level of strength and hardness.
- Adding copper to graphitized hypereutectoid steel leads to an increase in wear resistance in the conditions of sliding friction under boundary lubrication conditions.
- The reasons for the increase in mechanical properties are associated with the precipitation of ε-Cu phase particles (d ~20 nm).

1. Introduction

Currently, parts of sliding friction units of large-sized mechanisms, such as large excavators, e.g. sliding bushings (sometimes weighing more than 100 kg) are made of bronze. Replacing bronze in such units with less expensive materials is an urgent task. Copper-containing iron-carbon alloys are promising materials for replacing bronze in such large-sized components [1–13].

Research into the influence of copper on structural changes in iron-carbon alloys and its properties were conducted since the 1960s [8]. When iron-carbon alloys contain more than 2% copper, its tribological properties are enhanced. In practice, this is expressed in a decrease in the

friction coefficient and an increase in the wear resistance of the materials [1–13].

The main feature of such alloys is the presence of the ε-Cu phase, which precipitates in a wide range of sizes, starting from several nanometers [8, 10]. This is due to the fact that at room temperature the solubility of copper in iron is negligible. It is believed that almost all copper is contained in the form of the ε-Cu phase [7–10]. The low melting point of ε-Cu (1094 °C) makes it problematic to form the analyzed alloys in a hot state [14–16]. For this reason, parts made of antifriction iron-carbon alloys containing more than 3% Cu are usually manufactured by casting followed by heat treatment [8]. The limited scope of application explains the small amount of research on iron-carbon alloys with a high copper content. Most of the works are related to the analysis of the structure and properties of alloys containing less than 2% copper [1–13, 17–25] as well as its effect on corrosion resistance [26–30].

There are known antifriction materials based on iron, carbon and copper, obtained by powder metallurgy methods. Such materials have a high copper content and high antifriction properties, but the use of these materials in large, heavily loaded friction-sliding units is limited by their high cost and relatively low ultimate strength [31–33].

In the previous studies, special attention was paid to the classification of the particles of the ε-Cu phase; sections of the diagrams of the Cu–Fe–C system were given [9, 10, 17, 34].

The purpose of this work is to develop a cast antifriction material based on graphitized hypereutectoid steel with a high copper content for use in large, heavy-loaded sliding friction units.

2. Methods and materials

To obtain the materials under study, the technology of casting into self-hardening liquid glass molds was used. Foundry technologies were implemented at the Tsentrolit-S LLC enterprise in Novosibirsk. The metal was melted in an OKB-281 induction furnace with a crucible capacity of 750 kg. The castings were produced at an industrial scale under real production conditions. In the melting of the iron-carbon alloys, the volume of melt plays an important role. During the melting process, the material comes into contact with the crucible lining, becoming saturated with the elements present in it. The larger the volume of the furnace crucible, the fewer chemical elements and non-metallic inclusions get from the lining into the melt. The melting was carried out in a furnace with an acidic crucible lining. The metal was poured from a ladle with a capacity of 200 kg. Large volumes of metal in the ladle provided the same temperature conditions for all castings obtained during one experiment. The mass of each casting was 20 kg.

Steel 20 (0.2% C) and heat-treated graphite material (TU 1914-00194042-026-01) were used as burden materials. Steel and graphite material were the first components placed in the crucible in a solid state during the smelting process. Alloying elements were added to the melt. Before alloying elements addition, the melt was refined with liquid slag. The slag included quicklime (GOST 9179-77) and SiCa compound (GOST 4762-71).

In-mold modification of the melt was carried out with the SiCa compound (GOST 4762-71). When implementing this process, a package with a modifier was placed between two ceramic filters located in a sprue funnel and firmly fixed in it during the molding process.

The modifier concentration was calculated for 20 kg of melt (to obtain a concentration of 0.15 wt.%). The advantage of the noted solution is the absence of the possibility of the modifier floating up and the uniform distribution of particles in the melt.

Chemical analysis of the materials obtained during the experiments was carried out on an ARL-3460 optical emission spectrometer. The results of the analysis of castings are presented in Table 1 in mass percent.

The microstructural examination of cast materials were carried out using a Carl Zeiss Axio Observer A1m optical microscope, a Carl Zeiss EVO 50 XVP scanning electron microscope equipped with an EDSX-Act microanalyzer, and a FEI Technai G2 TWIN transmission electron microscope.

Evaluation of the distribution, shape, size and volume fraction of graphite was carried out on unetched sections. To analyze the phase composition, the specimens were subjected to chemical etching in a four percent alcohol solution of HNO_3 by dipping. Based on the analysis of the results of microstructural examination, the volume fraction and sizes of the phases were estimated. Particle sizes were determined with the ImageJ program by analyzing the images obtained using optical and transmission electron microscopes.

The phase analysis of the resulting alloys was studied using an ARL X'TRA θ-θ X-ray diffractometer. The source of X-ray radiation was a copper X-ray tube (voltage 40 kV, current 40 mA). The analysis of materials was carried out in the Bragg-Brentano geometry with no monochromator. The average beam wavelength λ recorded by the energy-dispersive Si(Li) detector was 0.15406 nm. Diffraction patterns were recorded in time mode (t = 1–5 s) with steps of $\Delta 2\theta$ = 0.02° and 0.05°.

The hardness of cast materials was measured using the Brinell method. The microhardness of individual phases was studied using the Vickers method using a Wolpert Group 402 MVD microhardness tester. The ultimate tensile strength of the materials was assessed by implementing two schemes (uniaxial static tension and compression of specimens) on a universal servo-hydraulic machine of the Instron 300 DX type.

Table 1 Elemental composition of castings.

Specimen	C	Mn	Si	P	S	Ni	Cr	Cu	Al
1	2.1	0.36	0.29	0.01	0.01	0.03	0.04	0.09	1.2
2	2.1	0.36	0.29	0.01	0.01	0.03	0.04	8.76	1.2

 DOI: 10.15826/chimtech.2023.10.3.15

Since the material under development will be used in sliding friction units (in particular, the material can be used for the manufacture of bushings) the most important indicators characterizing the tribological properties of such materials are the coefficient friction and wear resistance under sliding friction conditions. Based on the research results, the dependences of the sliding friction coefficient (μ) on the applied load were established. The value of μ was determined on an II5018 friction machine when implementing the liner-on-disk scheme in the presence of a lubricator – LUKOIL STANDART 10W-40 mineral oil. The shaft rotation frequency was 300 rpm. The specimens under study were segments cut from rings with an internal diameter of 50 mm and an external diameter of 68 mm. The width of the segments was 10 mm. The contact area between the disc and the liner was 20 mm².

The friction coefficient of the specimens was determined by the equation:

$$M = F/N, \quad (1)$$

where F – friction force, N – normal component of the external force, affecting the contact surface.

The wear resistance of materials under sliding friction conditions was determined using an SMT-1 friction machine using a plane-on-disk scheme. The load on the specimen (P) in all cases was the same – 500 N. The disk rotation frequency ω was 200 rpm. LUKOIL STANDART 10W-40 mineral oil was supplied to the friction zone. Disks made of hardened steel 45 (0.45% C) with a hardness of HRC 55, an outer diameter of 50 mm and a thickness of 10 mm, were used as counterbodies in the implementation of both schemes.

During the test, the length and width of the wear crater were measured. The level of wear resistance of materials was assessed by the volume of worn material, which was calculated using the formula:

$$V = S_{\text{circ.seg.}} l, \quad (2)$$

where l – wear crater width, $S_{\text{circ.seg.}}$ – area of a circle segment with a diameter of 50 mm, determined by the equation:

$$S_{\text{circ.seg.}} = 0.5R^2(\alpha - \sin\alpha), \quad (3)$$

where R = 25 mm - disk radius, α – circle sector angle:

$$\alpha = \arccos\alpha = (2R^2 - b^2)/2R^2, \quad (4)$$

where b – wear crater length.

3. Results and Discussion

3.1. The impact of copper on the structure of graphitized hypereutectoid steel

The microstructural examination shows that the addition of copper into graphitized hypereutectoid steel is accompanied by a change in the morphology of graphite inclusions. In the alloy with a minimum copper content (specimen 1), compact graphite predominates (Figure 1). Increasing the copper content in steel leads to a change in the shape of graphite from compact to vermicular. In the alloy containing 8.75% Cu (specimen 2), vermicular graphite is located in the interdendritic space and is represented by a mesh consisting of individual plates (Figure 2). The microstructural examination of graphitized hypereutectoid steel with 8.7% copper, carried out in the ImageJ software, showed that the average size of the graphite plates forming the mesh was ~5 μm.

The studies carried out in this work show that copper added to the alloys change not only the morphology and volume fraction of graphite inclusions, but also the structure of the metal base of the alloy.

In the absence of copper (specimen 1), the main structural components of the material are colonies of lamellar pearlite and inclusions of compact graphite. Some of the graphite inclusions are surrounded by ferrite rims (Figure 3). With the addition of 8.75% copper (specimen 2), ferrite does not occur in the cast iron structure (Figure 4). Aside from that, with the addition of more than 3% copper into the composition of the iron-carbon alloy, the dispersity of lamellar pearlite increases [34], which is confirmed in this study.

One of the most important features of the structure formation of Cu-alloyed iron-carbon alloys is associated with the presence of the ε-Cu phase in their structure. ε-Cu particles of two types (small particles of irregular shape with a size of 1–2 μm and large particles of spherical shape with a size of 8–70 μm) were detected in the structure of the alloy with 8.75% copper (specimen 2) using optical microscopy methods. Moreover, more than half of the particles volume fraction falls on the particles with a size of ~15–30 μm.

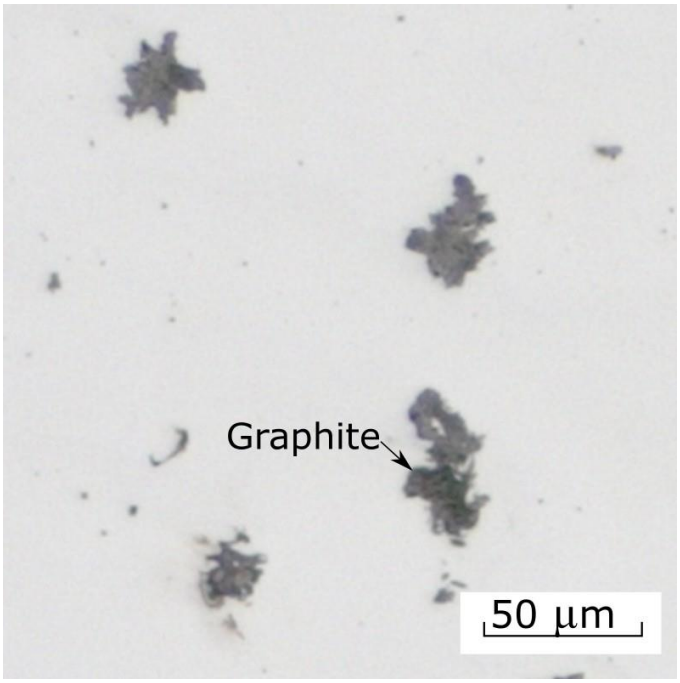

Figure 1 Compact graphite in the structure of graphitized steel (specimen 1).

 DOI: 10.15826/chimtech.2023.10.3.15

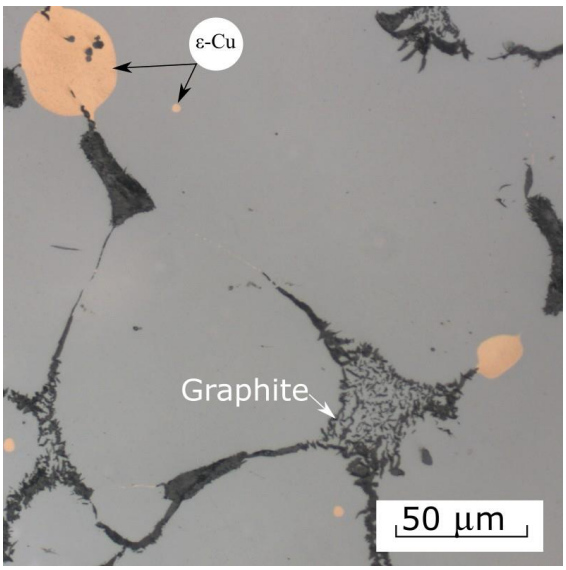

Figure 2 Vermicular graphite and ε-Cu phase in the structure of graphitized steel alloyed with copper (specimen 2).

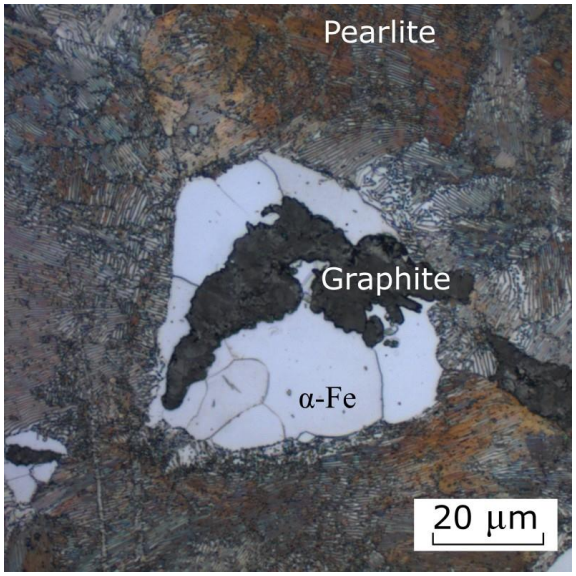

Figure 3 Structure of graphitized hypereutectoid steel (specimen 1).

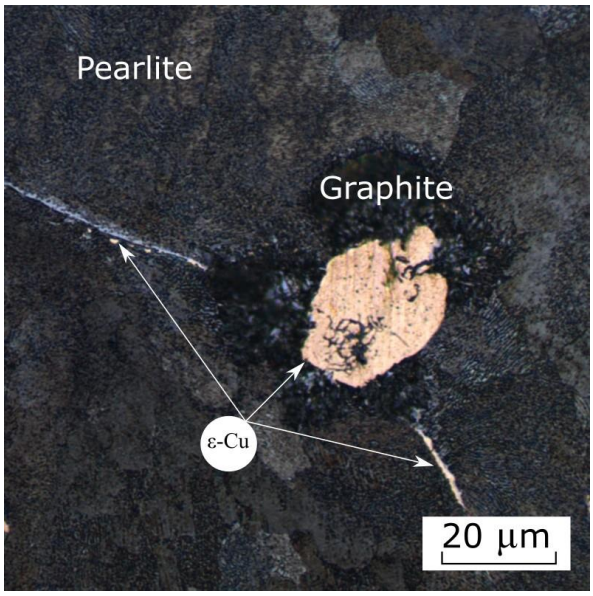

Figure 4 Structure of graphitized hypereutectoid steel alloyed with copper (specimen 2).

Large particles are distributed evenly throughout the entire body of the casting. Analysis of state diagrams of the Fe–C–Cu system [8, 15, 16, 35, 36] shows that with a copper content of ~9 wt.% large particles of the ε-Cu phase are formed from the melt. A melt of this composition is stratified into a liquid rich in iron and a liquid rich in copper. During the crystallization of the liquid rich in iron, the liquid rich in copper is pushed aside, and, subsequently, the largest particles of the ε-Cu phase are precipitated from it.

Particles with an average size of 1–2 μm are formed due to a decrease in the solubility of copper in austenite during its cooling. It is obvious that all the copper, which, in accordance with the phase diagram, should be precipitated from γ-Fe as the temperature of the alloy decreases, cannot be concentrated in the form of inclusions along the austenite boundaries. The volume of remaining copper, exceeding the limit of its solubility in austenite, is precipitated inside the austenite grains in the form of ε-Cu particles, the shape of which is close to spherical.

Using transmission microscopy methods, particles of the ε-Cu phase were detected, formed during a change in the solubility of copper in α-Fe. The average size of such particles is ~20 nm (Figure 5). Most of these particles are evenly distributed within the ferrite interspaces of pearlite. At the same time, the nature of some of the copper particles is associated with the a heterophase nucleation mechanism. Transmission electron microscopy detected particles precipitated on the surface of cementite perlite plates (Figure 5).

The results of X-ray diffraction analysis of the alloys under study are shown in Figure 6. Interpretation of the diffraction pattern of graphitized hypereutectoid steel with a minimum copper content (0.09%) indicates the presence of cementite, graphite and a solid solution based on α-Fe with a unit cell parameter of 2.872 Å in the alloy.

An increase in the copper content to 8.76% leads to an increase in the unit cell parameter of α-iron to 2.876 Å, as evidenced by a shift of the peaks towards smaller angles. The increase in the α-Fe parameter from 2.872 Å to 2.876 Å can be explained by the dissolution of copper in the ferritic matrix of the steel. It should be emphasized that most studies devoted to the analysis of alloys of the Fe-Cu system note an almost complete lack of solubility of copper in iron at room temperature [8, 15, 35].

It is possible that the signs of copper solubility in α-Fe observed in this work are due to the presence of 1.2% aluminum in the analyzed alloys.

In the material alloyed with 8.76% copper, peaks of the ε-Cu phase are detected. The unit cell parameter of this type of solid solution is 3.637 Å.

3.2. The impact of copper on the mechanical properties of graphitized hypereutectoid steel

Alloying graphitized hypereutectoid steel with copper causes a noticeable increase in the level of Brinell hardness from 246±3 to 298±7 HB, an increase in the ultimate tensile strength from 250±30 to 380±40 MPa and an increase

 DOI: 10.15826/chimtech.2023.10.3.15

in the level of ultimate compressive strength from 1050±30 to 1200±45 MPa. The increase in the level of strength indicators recorded in the work is explained by a number of factors. The impact of these factors is manifested in an increase in the microhardness of pearlite from 351±18 HV to 414±18 HV as the main structural component of all the alloys under study. The main reasons for the increase in the microhardness of lamellar pearlite are associated with an increase in the dispersion of the ferrite-cementite mixture, the precipitation of strengthening nano-sized copper particles ε-Cu (~ 20 nm) in the ferrite interspaces of the colonies as well as with the presence of dissolved copper atoms in α-iron.

In previous studies of hypereutectoid steels and cast irons alloyed with ~ 9% copper [9], it was found that the hardness of cementite does not depend on the copper content in the alloy, and it was concluded that the increase in the microhardness of pearlite is associated with changes in the ferrite included into the mechanical mixture. Among other factors, this is due to an increase in the volume fraction of the ε-Cu phase as well as the content of copper atoms dissolved in the α-Fe lattice. During the deformation of a Cu-alloyed material, nanosized inclusions are obstacles to moving dislocations, determining the hardness of pearlite and, as a consequence, the entire material. Figure 7 allows drawing a conclusion about the features of the distribution of dislocations in the alloy with finely dispersed copper particles contained in it. Most dislocations are attached to nearby particles of the ε-phase. Analysis of the structural features of the alloys under study suggests the possibility of implementing two mechanisms of interaction of dislocations with ε-Cu particles in it: the Orowan mechanism, according to which sliding dislocations bend around a particle, and the Hirsch mechanism, associated with transverse dislocation sliding. No dislocations cutting copper particles were detected, so there is no reason to consider hardening according to the Nicholson-Mott mechanism.

3.3. The impact of copper on the antifriction properties of graphitized hypereutectoid steel

The dependence of the friction coefficient on the applied specific load is assessed in the work. Figure 8 identifies three zones corresponding to the theoretical dependence [37, 38]. Analysis of the results obtained during testing indicates that at low loads the friction mode with lubrication is realized (zone 1, “transition mode”). In zone 2 (“stationary mode”) the friction coefficient has the lowest values. In this zone, the liquid friction mode is most often realized, in which the values of the friction coefficient depend on the characteristics of the lubricant, which in turn are related to the experimental conditions. In some cases, a boundary lubrication conditions may occur in this zone, depending not only on the properties of the lubricant, but also on the material from which the contacting surfaces are made. However, the extremely low values of the friction coefficient in this zone indicate the predominance of the impact of the lubricant properties.

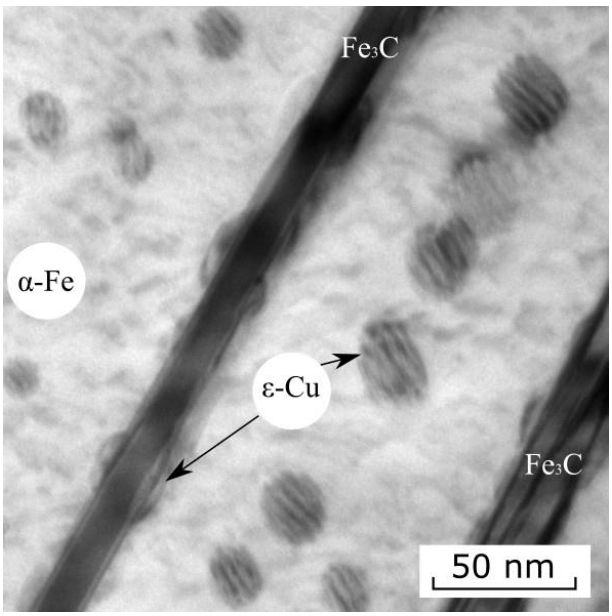

Figure 5 TEM images of graphitized hypereutectoid steel alloyed with copper (specimen 2)

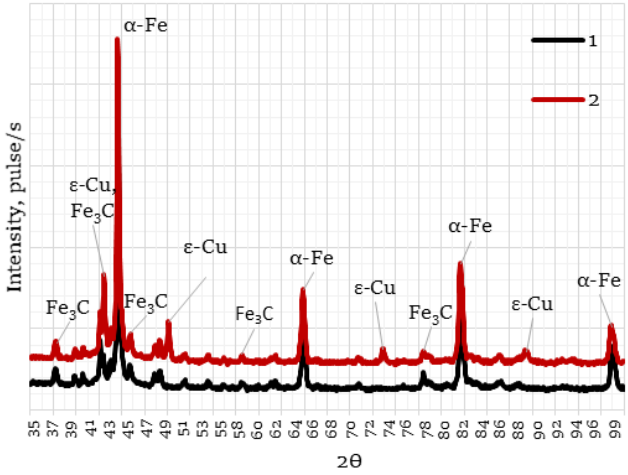

Figure 6 X-ray diffraction pattern of graphitized hypereutectoid steel without copper (1) and alloyed with copper (2)

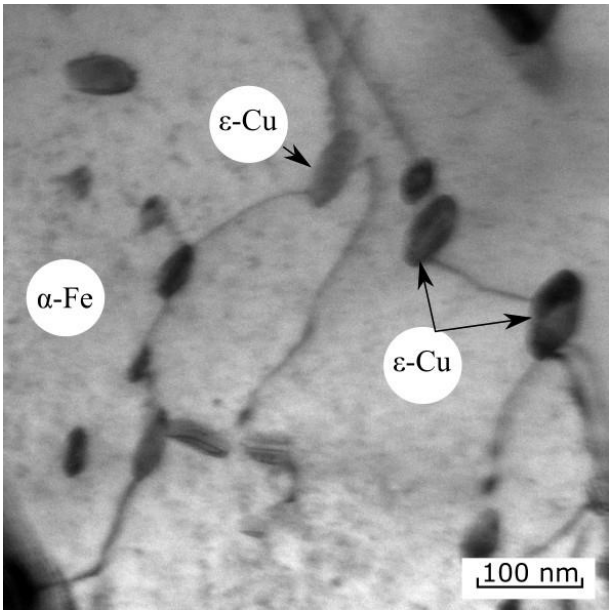

Figure 7 Features of dislocation distribution in the ferritic matrix of graphitized steel alloyed with copper

 DOI: 10.15826/chimtech.2023.10.3.15

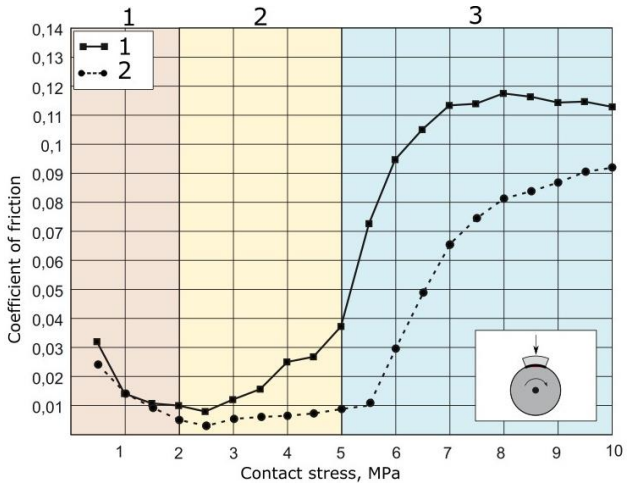

Figure 8 Impact of copper on the sliding friction coefficient of graphitized hypereutectoid steel.

Since the task is to determine the impact of copper on the antifriction properties of the materials under testing, comparison of specimens in zone 2 is irrelevant. In zone 3, with increasing specific load, a transition to the friction mode with boundary lubrication occurs. A further increase in load can lead to complete squeezing out of the lubricant from the friction zone and the implementation of the "friction without lubricant" conditions.

The peculiarity of the steels under study (as in the previous series of experiments) was that in addition to copper, its composition also included aluminum. It should be noted that in the structure of Al-alloyed iron-carbon alloys and containing ≥6% Cu, copper-containing inclusions are formed, the chemical composition of which is close to the composition of BrA9Zh3L bronze [38]. The presence of such inclusions is probably one of the most significant factors explaining the improvement in tribological properties upon joint alloying of steel with copper and aluminum.

With a friction path length of ~ 13 km, the volume of worn material with the addition of copper into the steel composition decreased by 1.5–2 times (from 0.018 mm_3 for a specimen without copper to 0.0095 mm_3 for a specimen containing copper); that is, the wear resistance of the material under sliding friction conditions increased. The reasons for such behavior of the analyzed materials are associated with an increase in hardness and a decrease in the sliding friction coefficient with an increase in copper content. The combined impact of both factors has a beneficial effect on the behavior of hypereutectoid steels operating under conditions of sliding friction.

4. Limitation

This study shows the results of the influence of copper on the structure and properties of cast graphitized steel. The next logical stage in the development of the material is to evaluate the influence of copper on the structures and properties of iron-carbon alloys under various heat treatment modes.

5. Conclusions

In the course of the research, the following conclusions were made:

1. Alloying graphitized hypereutectoid steel with 8.76% copper leads to enhanced mechanical properties, namely, an increase in the Brinell hardness level of the material from 250 to 300 HB, an increase in ultimate tensile strength from 250 to 380 MPa and an increase in the level of ultimate strength at compression from 1050 to 1200 MPa, as well as an increase in the microhardness of the main structural component – pearlite – from 350 to 420 HV.
2. The main reasons for the increase in the microhardness of lamellar pearlite are associated with an increase in the dispersity of the ferrite-cementite mixture, the precipitation of strengthening nano-sized copper particles ε-Cu (~ 20 nm) in the ferrite interspaces of the colonies, and with the presence of dissolved copper atoms in α-iron.
3. Alloying graphitized hypereutectoid steel with 8.76% copper leads to a decrease in the level of sliding friction coefficient under conditions of boundary lubrication as well as to an increase in the wear resistance of the material under conditions of sliding friction.

• Supplementary materials

No supplementary materials are available.

• Funding

This research had no external funding.

• Acknowledgments

Research was conducted at the core facility "Structure, mechanical and physical properties of materials".

• Author contributions

Conceptualization: N.V.S.
Optical metallography, TEM, SEM: N.V.S., L.E.A.
Mechanical properties: N.V.S.
Anti-friction properties: N.V.S.
Data curation: N.V.S., L.E.A.
Investigation: N.V.S.
Methodology: N.V.S.
Resources: N.V.S.
Supervision: N.V.S.
Writing – original draft: N.V.S.
Writing – review & editing: N.V.S., L.E.A.

• Conflict of interest

The authors declare no conflict of interest.

 DOI: 10.15826/chimtech.2023.10.3.15

• Additional information

Author IDs:

Natalia V. Stepanova, Scopus ID 55933634800;

Elena A. Lozhkina, Scopus ID 56433383400.

Website:

Novosibirsk State Technical University, https://en.nstu.ru/.

References

1. Osterle W, Prietzel C, Kloss, Dmitriev A. On the role of copper in brake friction materials. Tribol Int. 2010;43:2317–2326. doi:10.1016/j.triboint.2010.08.005
2. Agunsoye JO, Bello SA, Hassan SB, Adeymo RG, Odii JM. The effect of copper addition on the mechanical and wear properties of grey cast iron. J Minerals Mater Characteriz Engin. 2014;2(5):470–483. doi:10.4236/jmmce.2014.25048
3. Zhang B, Xu B, Xu Yi. Cu nanoparticles effect on the tribological properties of hydrosilicate powders as lubricant additive for steel-steel contacts. Tribol Int. 2011;44(7):878–886. doi:10.1016/j.triboint.2011.03.002
4. Zhai W, Lu W, Liu X. Nanodiamond as an effective additive in oil to dramatically reduce friction and wear for fretting steel/copper interfaces. Tribol Int. 2019;129:75–81. doi:10.1016/j.triboint.2018.08.006
5. Rodrigues ACP, Oesterle W, Gradt T. Impact of copper nanoparticles on tribofilm formation determined by pin-on-disc tests with powder supply: Addition of artificial third body consisting of Fe_3O_4, Cu and graphite. Tribol Int. 2017;110:103–112. doi:10.1016/j.triboint.2017.02.014
6. Eroglu M. Boride coatings on steel using shielded metal ARC welding electrode: microstructure and hardness. Surface Coatings Technol. 2009;203:2229–2235. doi:10.1016/j.surfcoat.2009.02.010
7. Silman GI, Kamynin VV, Goncharov VV. On the mechanisms of copper effect on structure formation in cast iron. Metal Sci Heat Treatment. 2007;48(7–8):387–393. doi:10.1007/s11041-007-0072-z
8. May IL, Schetky LD. Copper in iron and steel. New York: Wiley Interscience; 1982. 423 p.
9. Bataev AA, Stepanova NV, Bataev IA, Kang Y, Razumakov AA. Special features of precipitation of ε-Cu phase in cast irons alloyed with copper and aluminum. Metal Sci Heat Treat. 2018;60(3–4):150–157. doi:10.1007/s11041-018-0253-y
10. Stepanova NV, Bataev IA, Kang Y, Lazurenko DV, Bataev AA, Razumakov AA, Jorge Junior AM. Composites of copper and cast iron fabricated via the liquid: In the vicinity of the limits of strength in a non-deformed condition. Mater Characteriz. 2017;130:260–269. doi:10.1016/j.matchar.2017.06.025
11. Upadhyay S, Saxena KK. Effect of Cu and Mo addition on mechanical properties and microstructure of grey cast iron: An overview. Mater Today Proc. 2020;26(2):2462–2470. doi:10.1016/j.matpr.2020.02.524
12. Sazegaran H, Teimoori F, Rastegarian H, Naserian-Nik AM. Effects of aluminum and copper on the graphite morphology, microstructure, and compressive properties of ductile iron. J Mining Metallurgy Sec B Metallurgy. 2021;57(1):145–154. doi:10.2298/JMMB191224006S
13. Garcia LN, Tolley AJ, Carazo FD, Boeri RE. Identification of Cu-rich precipitates in pearlitic spheroidal graphite cast irons. Mater Sci Technol. 2019;35(18):2252–2258. doi:10.1080/02670836.2019.1668999
14. Sil'man GI, Kamynin VV, Tarasov AA. Effect of copper on structure formation in cast iron. Metal Sci Heat Treat. 2003;45(7–8):254–258. doi:10.1023/A:1027320116132
15. Shubhank K, Kang Y. Critical evaluation and thermodynamic optimization of Fe–Cu, Cu–C, Fe–C binary systems and Fe–Cu–C ternary system. Calphad. 2014:45127–45137. doi:10.1016/j.calphad.2013.12.002
16. Sil'man GI. About retrograde solidus and stratification of melt in the Fe–Cu and Fe–Cu–C systems. Metal Sci Heat Treat. 2009;51(1–2):19–24. doi:10.1007/s11041-009-9120-1
17. Lazurenko DV, Alferova GI, Emurlaev KI, Emurlaeva YY, Bataev IA, Ogneva TS, Ruktuev AA, Stepanova NV, Bataev AA. Formation of wear-resistant copper-bearing layers on the surfaces of steel substrates by non-vacuum electron beam acladding using powder mixtures. Surface Coatings Technol. 2020;395:125927. doi:10.1016/j.surfcoat.2020.125927
18. Zhang GW, Kang YY, Wang MJ, Xu H, Jia HM. Atomic diffusion behavior and diffusion mechanism in Fe–Cu bimetal casting process studied by molecular dynamics simulation and experiment. Mater Res Express. 2020;7:096519. doi:10.1088/2053-1591/abb90f
19. Chen K, Chen X, Wang Z, Sandstrom HMR. Optimization of deformation properties in as-cast copper by microstructural engineering. Part I. Microstructure. J Alloys Compd. 2018:763:592–605. doi:10.1016/j.jallcom.2018.05.297
20. Buck DM. Copper in steel – the influence on corrosion. J Indust Engin Chem. 1913;5(6)447–452. doi:10.1021/ie50054a003
21. Li B, Qu H, Lang Y. Copper alloying content effect on pitting resistance of modified 00Cr20Ni18Mo6CuN super austenitic stainless steels. Corrosion Sci. 2020;173:108791. doi:10.1016/j.corsci.2020.108791
22. Sun XY, Zhang B, Wu B, Wei XX, Oguzie EE, Ma XL. Investigating the effect of Cu-rich phase on the corrosion behavior of Super 304H austenitic stainless steel by TEM. Corrosion Sci. 2018;130:143–152. doi:10.1016/j.corsci.2017.11.001
23. Zhang, ZX, Lin G, Xu Z Effects of light pre-deformation on pitting corrosion resistance of copper bearing ferrite antibacterial stainless steel. J Mater Proc Technol. 2008;205:419–424. doi:10.3390/ma13020403
24. Jeon S, Kim S, Lee I, Park J, Kim K, Kim J, Park Y. Effects of copper addition on the formation of inclusions and the resistance to pitting corrosion of high performance duplex stainless steels. Corrosion Sci. 2011;53:1408–1416. doi:10.1016/j.corsci.2011.01.005
25. Zhang J, Young DJ. Effect of copper on metal dusting of austenitic stainless steels. Corrosion Sci. 2007;49:1450–1467. doi:10.1016/j.corsci.2006.06.032
26. Hsu Ch, Lin K. Effects of copper and austempering on corrosion behavior of ductile iron in 3.5 PCT sodium chloride. Metallurg Mater Trans A Phys Metallurg Mater Sci. 2014;45:3:1517–1523. doi:10.1007/s11661-013-2059-2
27. Seo M, Hultquist G, Leygraf C, et al. The influence of minor alloying elements (Nb, Ti and Cu) on the corrosion resistivity of ferritic stainless steel in sulfuric acid solution. Corros Sci., 1986;26(949–955):957–960. doi:10.1016/0010-938X(86)90085-5
28. Gong L, Fu H, Zhi X. First-principles study on corrosion resistance of copper-bearing hypereutectic high chromium cast iron. Mater Today Commun. 2022;33:104345. doi:10.1016/j.mtcomm.2022.104345
29. Wei M, Yang B, Liu Y, et al. Research progress and prospect on erosion-corrosion of Cu-Ni alloy pipe in seawater. J Chinese Soc Corros Protect. 2016;36(6):513–521. doi:10.11902/1005.4537.2016.123
30. Sandra N, et al. Influence of copper slag on corrosion behavior of horizontal steel bars in reinforced concrete column specimen due to chloride-induced corrosion. Construc Build Mater. 2020;255:119265. doi:10.1016/j.conbuildmat.2020.119265
31. Aperador W, Bautista-Ruiz J, Caicedo J. Wear synergy of copper-iron mixtures processed by powder metallurgy. Rasayan J Chem. 2021:193–199. doi:10.31788/RJC.2021.1456678
32. Lapierre-Boire L-P, Blais C, Pelletier S, Chagnon F. Improvement of flow of an iron-copper-graphite powder mix through additions of nanoparticles. Powder Technol. 2016;299:156–167. doi:10.1016/j.powtec.2016.05.046

 DOI: 10.15826/chimtech.2023.10.3.15

33. Fedorchenko IM, Pugina LI. Kompozitsionnyye spechennyye antifriktsionnyye materialy [Composite sintered antifriction materials]. Kyiv: Nauk, Dumka, 1980. 404 p.
34. Bataev IA, Stepanova NV, Bataev AA, Nikulina AA, Razumakov AA. Peculiarities of the precipitation of nanosized ε-phase copper particles in ferrite plates of lamellar pearlite. Phys Metals Metallograph. 2016;117(9):901–905. doi:10.1134/S0031918X16090015
35. Shubhank K, Kang Y. Critical evaluation and the termodynamic optimization of Fe–Cu, Cu–C, Fe–C binary systems and Fe–Cu–C ternary system. Calphad. 2014;45:127–137. doi:10.1016/j.calphad.2013.12.002
36. Stepanova NV, Mikhalev RI, Tarasova TD. Peculiarities of copper precipitation in hypereutectoid steels. Metallurg. 2023;66(11–12):1388–1400. doi:10.1007/s11015-023-01454-y
37. Chichinadze AV, Brown ED, Boucher NA. Basics of tribology (friction, wear, lubrication). 2nd ed. processing, and additional [Basics of tribology (friction, wear, lubrication). 2nd ed. processing, and additional] Moscow: Mechanical engineering; 2001. 664 p. Russian.
38. Kragelsky IV. Friction and wear. Edition 2, revised and expanded [Friction and wear. Edition 2, revised and expanded] Moscow: Mechanical engineering; 1968. 480 p. Russian.

 DOI: 10.15826/chimtech.2023.10.3.15